

JUL 17 1958

~~CONFIDENTIAL~~

Copy 1
RM L58D25a

NACA RM L58D25a

CLASSIFICATION CANCELLED

AUTHORITY CLASSIFICATION CHANGE NOTICE NO. 3 MAY 1 1968

DATE 9/9/68 BY Nelson

NACA

RESEARCH MEMORANDUM

HEAT-TRANSFER MEASUREMENTS ON A CONCAVE HEMISPHERICAL
NOSE SHAPE WITH UNSTEADY-FLOW EFFECTS AT

MACH NUMBERS OF 1.98 AND 4.95

By Morton Cooper, Ivan E. Beckwith, Jim J. Jones,
and James J. Gallagher

Langley Aeronautical Laboratory
Langley Field, Va.

PLEASE RETURN TO
DIVISION OF RESEARCH INFORMATION
NATIONAL ADVISORY COMMITTEE
FOR AERONAUTICS
Washington 25, D. C.

CLASSIFIED DOCUMENT

This material contains information affecting the National Defense of the United States within the meaning of the espionage laws, Title 18, U.S.C., Secs. 793 and 794, the transmission or revelation of which in any manner to an unauthorized person is prohibited by law.

NATIONAL ADVISORY COMMITTEE FOR AERONAUTICS

WASHINGTON

July 17, 1958

~~CONFIDENTIAL~~



NATIONAL ADVISORY COMMITTEE FOR AERONAUTICS

RESEARCH MEMORANDUM

HEAT-TRANSFER MEASUREMENTS ON A CONCAVE HEMISPHERICAL
NOSE SHAPE WITH UNSTEADY-FLOW EFFECTS AT
MACH NUMBERS OF 1.98 AND 4.95*

By Morton Cooper, Ivan E. Beckwith, Jim J. Jones,
and James J. Gallagher

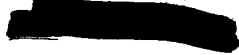
SUMMARY

16241

Heat-transfer rates and pressure fluctuations at Mach numbers of 1.98 and 4.95 have been measured at the stagnation point of a concave hemisphere for a Reynolds number range from 2×10^6 to 11×10^6 based on free-stream conditions and model diameter. These data, together with schlieren studies made at a Mach number of 1.98, show that for angles of attack less than approximately 2° either of two flow conditions could occur at both Mach numbers. The flow was observed to alternate in a random manner from steady flow to unsteady flow. The heat-transfer coefficients measured for the unsteady flow were approximately 6 to 7 times the coefficients for the steady flow. The ratio of the coefficients for the steady flow to the theoretical values at the stagnation point of a convex hemisphere varied from 0.2 to 0.5. At angles of attack of about 2° or more the heat-transfer rates were at the low level.

INTRODUCTION

The study of reentry shapes and methods for reducing heat transfer to such shapes has been the subject of intensive research. Recently, considerable interest has been stimulated in a concave hemispherical nose shape because of extremely low heating rates observed during exploratory tests (ref. 1). Values of stagnation-point heat-transfer rates about one-third those of the convex hemisphere were quoted for Mach numbers of about 3 and values as low as one-tenth for Mach numbers near 8. Additional tests at a Mach number of 2 (ref. 2) indicated values of 45 percent of those of the hemisphere. Lower stagnation-point heating rates on concave shapes than on convex shapes should be anticipated because of the smaller stagnation-point velocity gradient on the concave shape as indicated in reference 3 and measured in reference 4.

*Title, Unclassified. 


Subsequent to the investigations reported in reference 1 and 2, some unpublished data obtained by the Langley Pilotless Aircraft Research Division on rocket-propelled models indicated values of only one-eighth to one-twentieth of those on the hemisphere in the Mach number range from 3 to 7. Although in all cases (refs. 1 and 2 and the unpublished data) the stagnation-point heat transfer was less than that on the hemisphere, the apparently large differences in these data could not be explained. In an attempt to understand the phenomena causing these differences, an investigation was undertaken in the Gas Dynamics Branch of the Langley Laboratory to study further the concave hemisphere shape. The investigation was conducted at Mach numbers of 1.98 and 4.95 and Reynolds numbers, based on diameter and free-stream conditions, varying from 2×10^6 to 11×10^6 . The purpose of the present paper is to present some results of this investigation. While these results are considered preliminary, they are presented at this time because of the occurrence of an important phenomenon not previously observed in references 1 and 2 and the unpublished data. Although heat-transfer coefficients considerably lower than those obtained on a convex hemisphere have been measured at the stagnation point, values several times those of the hemisphere have also been obtained. The low values are associated with steady flow while the high values are associated with unsteady asymmetrical flow. Subsequent to the completion of these tests, both types of flow, together with the associated high and low heating rates, have also been observed in the Langley Unitary Plan wind tunnel. Hence, until the flow instability can be better understood or controlled, it should be assumed that the high heat rate is possible in practical applications.

SYMBOLS

q	heat-transfer rate per unit area
T_o	stagnation temperature
T_w	wall temperature
h	stagnation-point heat-transfer coefficient, $\frac{q}{T_o - T_w}$
h_s	theoretical stagnation-point heat-transfer coefficient for a convex hemisphere
R_d	Reynolds number based on free-stream conditions and model diameter

M	free-stream Mach number
α	angle of attack, deg
P_0	stagnation pressure, lb/sq in. abs

APPARATUS AND METHOD

Model

The heat-transfer model, which is shown in figure 1, was constructed from 17-4 PH stainless steel. The model was $1\frac{3}{4}$ inches in diameter and had a nominal skin thickness of 0.028 inch. In order to expedite these exploratory tests, only two iron-constantan thermocouples were installed on the inner surface of the model. One was located on the axis of symmetry and the other was located approximately as shown in figure 1. (The thermocouple located on the axis of symmetry will be designated herein as the stagnation-point thermocouple.) The measured skin thicknesses at the thermocouple locations were 0.025 inch for the axis of symmetry and 0.031 inch for the off-axis location. Only stagnation-point heat-transfer data will be presented.

A pressure model was tested to determine the pressure fluctuations at the stagnation point. The exterior shape and dimensions of this model were the same as those of the heat-transfer model (fig. 1). The pressure instrumentation consisted of a quartz piezoelectric pressure transducer. The diameter of the sensitive element was about $1/4$ inch.

Tunnels

Two blowdown tunnels in the Langley Gas Dynamics Laboratory were used for the tests. Both tunnels utilized dry air stored at 5,000 lb/sq in. in a common 20,000-cubic-foot storage system. The tests at $M = 1.98$ were conducted in an open 9- by 9-inch test section in the flow produced by a two-dimensional nozzle. The stagnation pressures varied from 90 to 170 lb/sq in. abs and the stagnation temperatures ranged up to 150° F. The initial model wall temperature ranged from 50° to 70° F.

The tests at $M = 4.95$ were conducted in a closed, axially symmetric test section, 9 inches in diameter. The stagnation pressure ranged from 500 to 2,500 lb/sq in. abs, and the stagnation temperature was approximately 400° F. The initial model wall temperature was about 75° F.

Installation

For both Mach numbers, the model, which was sting supported (as shown in fig. 2), was inserted by means of air-actuated cylinders into the airstream after steady-flow conditions were obtained. For the test at $M = 1.98$ the model was rotated into the stream about an axis parallel to the tunnel center line (fig. 2(a)). For the test at $M = 4.95$ the model was pushed into the tunnel in a horizontal plane (fig. 2(b)). (The model shown in figure 2(b) is not the one tested in the present investigation.) In order to accomplish this, a side door on the tunnel was lowered and then the model was inserted. The model-support system was mounted to a door which closed the tunnel as the model became centered (fig. 2(b)). For both Mach numbers the time required to bring the model into test position was a small fraction of a second.

Data Reduction

The heat-transfer data were evaluated by the transient calorimeter technique whereby the heat entering the model skin is equated to the heat stored. Because of the exploratory nature of the tests whereby trends and magnitudes were being studied, a simple one-dimensional heat balance assuming infinite skin conductivity in the direction normal to the wall was used, with lateral conduction neglected. The resulting heat-transfer coefficients, therefore, will be too low for two reasons. The geometry correction due to the concave hemispherical shape would increase the measured heat transfer by about 3 percent. An approximate analysis based on the one-dimensional unsteady heat-conduction equation for a wall of finite thickness (ref. 5) shows that an error of the order of 10 percent occurs at the highest coefficients since the thermocouples were located on the inner surface of the skin. It is not possible to evaluate reliably the lateral conduction correction without more detailed temperature-distribution data, but estimates based on the two thermocouples indicate that this effect would not be significant, at least for the earliest times.

RESULTS AND DISCUSSION

Heat-Transfer Records

Inasmuch as the heat-transfer records obtained during this investigation were quite unusual, and in many cases differed markedly for different runs, a representative series of the temperature-time records is presented in figures 3 to 5. In these figures multichannel-galvanometer records are presented for $M = 1.98$ and $\alpha = 0$ (fig. 3), for $M = 4.95$ and $\alpha = 0$ (fig. 4), and for angles of attack at both Mach numbers



(fig. 5). Temperature and time scales have been indicated on all records. The unlabeled temperature time history is that of the thermocouple located off the axis. It is to be noted that a separate base line exists for each galvanometer channel. For the tests at $M = 1.98$, the stagnation temperature was recorded directly with the other thermocouples. For the tests at $M = 4.95$, however, the stagnation temperature was recorded on a self-balancing potentiometer. For some of the $M = 4.95$ records, a static pressure on the tunnel wall, near the model, is shown to verify that the tunnel has "started" and uniform flow has been established. The first rise in the static-pressure record (fig. 4(a)) occurs when the tunnel is opened to atmosphere so that the model can be inserted into the tunnel. The drop occurs when the tunnel is closed as the model is inserted. Although flow in the tunnel is reestablished almost immediately, the relatively slow response time of the orifice installation accounts for the slow drop in pressure to the tunnel-empty value.

The two temperature-time records shown in figure 3 for $M = 1.98$ are for essentially the same stagnation conditions. The higher heating rate (fig. 3(a)) is approximately six times the lower rate (fig. 3(b)). This surprising result whereby either of two considerably different heat-transfer rates may occur is due to the existence of two basically different flow patterns as will become more evident subsequently. (The rapid rise in temperature occurring for the first 0.2 second, fig. 3(b), of the initial heating period for this particular test is extraneous and is associated with the entrance of the model into the airstream.) It is of interest to note that the high heat-transfer rate drops sharply (fig. 3(a)) after about 3.8 seconds. There is insufficient precision at this point, however, to evaluate the heat-transfer coefficient.

The temperature-time records for $M = 4.95$ (fig. 4) show similar and even more irregular occurrences. For example, at a stagnation pressure of 1,020 lb/sq in. abs (fig. 4(b)), the heating rate oscillates simultaneously for both thermocouples from high to low values as the flow pattern changes. Similar oscillations were also obtained in a more or less random pattern during other tests at both Mach numbers. In another test (fig. 4(a)) at approximately the same stagnation conditions as those of figure 4(b) only the high rate was observed. In the records obtained at stagnation pressures of 2,535 and 1,515 lb/sq in. abs (figs. 4(c) and 4(d)), the high heating rates were observed initially. However, after about 0.3 second there was a nearly discontinuous change in the temperature-time slope for 2,535 lb/sq in. abs. The heat-transfer coefficient just after the change in slope is about one-sixth the value during the first portion of the record. These changes in heat-transfer rates are again associated with changes in the flow pattern. It should be noted that the cooling indicated after peak temperature (fig. 4(b)) was caused by retracting the model from the tunnel.



In the present tests at angle of attack (fig. 5) the records were smooth and in all cases exhibited low heat-transfer rates. It should be noted, however, that on one occasion in the Langley Unitary Plan wind tunnel the high heating rate was measured at an angle of attack of $7\frac{1}{2}^{\circ}$ at $M = 2.5$.

Heat-Transfer Data

Heat-transfer data for two oscillating-flow-condition tests at $M = 4.95$ and essentially the same stagnation conditions are presented in figure 6. In this figure and in figure 7 the heat-transfer coefficient has been referenced to the theoretical value at the stagnation point of a convex hemisphere (ref. 6), assuming a Newtonian velocity gradient for the hemisphere. The oscillation of the flow from high to low rate is aperiodic.

In figure 7 all the stagnation-point heat-transfer data have been summarized. All the symbols except the squares denote separate tests. Square symbols indicate that both high and low values occurred during a given test. One average high value and one average low value are presented for the oscillating-flow test shown in figure 6. Clearly for both Mach numbers the data subdivide into two heating levels. In general, the low level varies from 20 to 50 percent of the hemisphere and the high level is about 6 or 7 times the low value. For these data there is roughly a 50-percent increase in both the high and the low heating rates as the Reynolds number is increased. Laminar boundary-layer theory would predict h/h_g independent of Reynolds number. The off-axis thermocouple indicated heat-transfer values approximately equal to or somewhat less than those indicated by the stagnation-point thermocouple. The stagnation-point value quoted in reference 2 and shown in figure 7 is consistent with the low heating rates observed in the present tests. There is, however, no explanation for the difference between these results and those from the unpublished rocket test ($M = 3$ to $M = 7$), which were approximately one-fourth the low rates shown for $M = 4.95$ at corresponding Reynolds numbers.

At angles of attack of approximately 2° or greater the low heat rate always occurred in the present tests.

Schlieren Photographs and Stagnation Point

Pressure Measurements

In order to obtain a better understanding of the phenomena associated with the high and low heating rates, a series of schlieren



photographs and stagnation point pressure measurements were made. The schlieren pictures were obtained at $M = 1.98$ and the pressure measurements were made at $M = 1.98$ and $M = 4.95$.

Typical schlieren photographs are presented in figure 8. Photographs taken with and without flow in the empty tunnel are shown for reference purposes. Figures 8(c) and 8(d) illustrate one flow configuration, while figures 8(e) and 8(f) illustrate the other flow configuration. (A photographic highlight in figures 8(e) and 8(f) obscures the leading edge of the model.) With the aid of additional schlieren pictures such as these, coupled with the thermocouple records and the piezoelectric measurements of pressure, it is possible to classify the types of flow as follows:

- (a) Steady flow and low heat transfer
- (b) Unsteady flow and high heat transfer

Steady flow.- Steady flow and low heat transfer are characterized by a shock wave which is symmetric at zero angle of attack and relatively close to the body as shown in figures 8(c) and 8(d). Motion pictures taken at 2,000 frames per second indicated that the bow shock was steady. For this condition, the piezoelectric pressure transducer indicated only a slight pressure oscillation as illustrated for $M = 4.95$ in figure 9. The pressure corresponded to the stagnation pressure behind a normal shock. This steady flow was observed during all the present tests for angles of attack greater than about 2° and intermittently for angles of attack less than about 2° .

Unsteady flow.- For angles of attack of the order of 2° or less, an alternate flow characterized by an asymmetric bow shock and high heat-transfer rate was also observed. As can be seen in figures 8(e) and 8(f), the shock is considerably farther ahead of the body than for the symmetrical low-heat-transfer case. The air inside the concave nose appears to spill alternately around different sides of the body. At 2,000 frames per second the asymmetric shock for $M = 1.98$ is primarily steady with superposed bursts of unsteadiness. For this Mach number there was no discernible change in frequency of pressure fluctuation as the flow shifted from steady to unsteady. At $M = 4.95$, however, the stagnation-point pressure (fig. 9) showed a high-frequency fluctuation of the order of 2,000 cycles per second. (Inasmuch as the natural frequency of the recording system was only about 1,000 cycles per second, the amplitudes of the fluctuations, which might include some mechanical effects, were attenuated.) These high-frequency pressure fluctuations are consistent with unpublished schlieren observations at $M = 4.5$ in the Langley Unitary Plan wind tunnel. In those tests, the shock fluctuated violently and almost continuously for the unsteady flow. There seems to be a Mach number effect whereby the unsteadiness occurs more readily and

becomes more violent at high Mach numbers. The mean of the pressure fluctuations (fig. 9) corresponds to a pressure about 15 percent greater than the stagnation pressure behind a normal shock. The increase in pressure is probably due to the asymmetrical shock, inasmuch as a similar increase was noted at $M = 1.98$. During the pressure tests the flow was observed to oscillate between the two conditions sometimes in less than 0.1 second and other times requiring many seconds.

Although the high heat rate and unsteady flow are shown for only one Reynolds number at $M = 1.98$ (figs. 7, 8(e), and 8(f)) when schlieren and heat-transfer records were obtained simultaneously, the unsteady flow was observed over the complete Reynolds number range during schlieren studies alone.

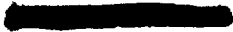
Although the unsteady flow was never observed for angles of attack greater than approximately 2° during the present tests, the high heating rate was measured during one test at $M = 2.5$ and $\alpha = 7\frac{1}{2}^\circ$ in the Langley Unitary Plan wind tunnel. During one other test in the Langley Unitary Plan wind tunnel at $M = 4.5$ and $\alpha = 15^\circ$, the unsteady shock was observed in the schlieren pictures.

General Remarks

These tests have clearly established that two flow configurations can occur on a concave hemispherical nose, and that the heating rates may be either higher or lower than the heating rates for the convex hemisphere. Before any further recommendations are made regarding the practical use of this configuration, it will be necessary to better understand or control the flow. On the basis of some exploratory tests it appears possible to assure the low-heat-transfer conditions by changing the relative proportions or modifying the contour of the internal concave regions.

CONCLUDING REMARKS

Heat-transfer rates and pressure fluctuations at Mach numbers of 1.98 and 4.95 have been measured at the stagnation point of a concave hemisphere for a Reynolds number range from 2×10^6 to 11×10^6 based on free-stream conditions and model diameter. These data and schlieren photographs obtained during the same tests show that for angles of attack less than approximately 2° either of two flow conditions could occur. The flow was generally observed to alternate in a random manner from steady flow to unsteady flow.



For the unsteady flow, the pressure at the stagnation point fluctuated at a frequency of the order of 2,000 cycles per second at a Mach number of 4.95 and the mean of the pressure fluctuations corresponded to a pressure about 15 percent greater than the stagnation pressure behind a normal shock for both Mach numbers. No significant fluctuations were observed for the steady flow.

For the steady flow, the bow shock wave was symmetrical at zero angle of attack and relatively close to the body. For the unsteady flow the shock wave was asymmetrical and much farther ahead of the body.

The heat-transfer coefficients measured for the unsteady configuration were approximately 6 to 7 times the coefficients for the steady flow. The steady-flow coefficients varied from 20 percent to 50 percent of the values at the stagnation point of a convex hemisphere.

At angles of attack of about 2° or more, only low heat-transfer rates were obtained during these tests.

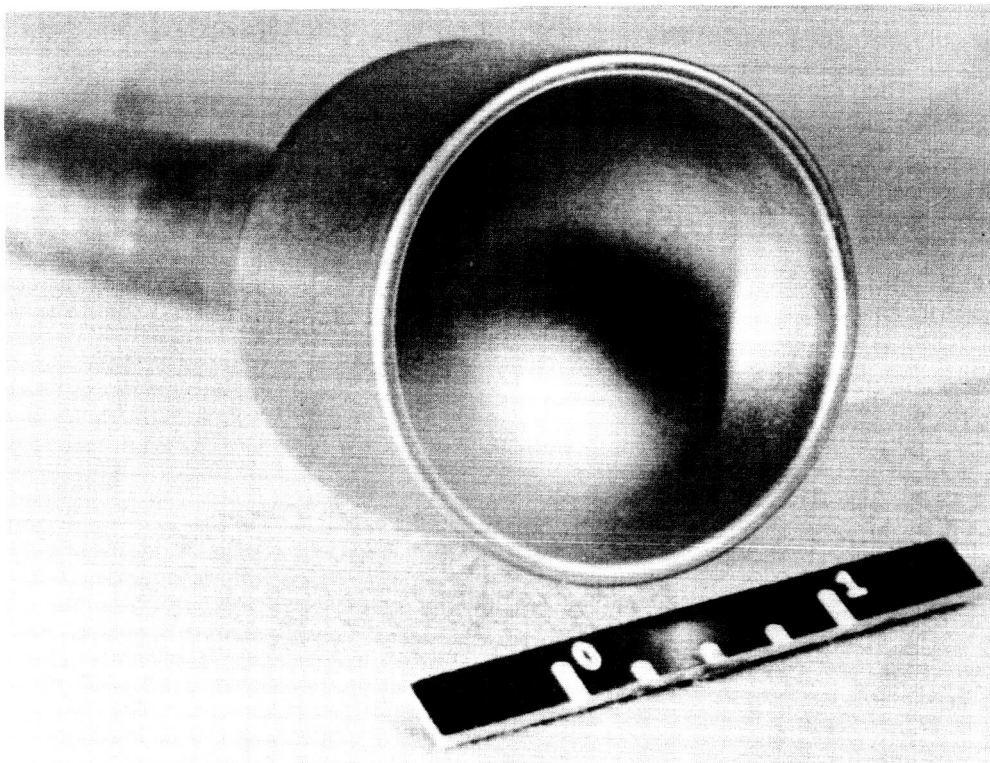
Langley Aeronautical Laboratory,
National Advisory Committee for Aeronautics,
Langley Field, Va., April 11, 1958.

CONFIDENTIAL



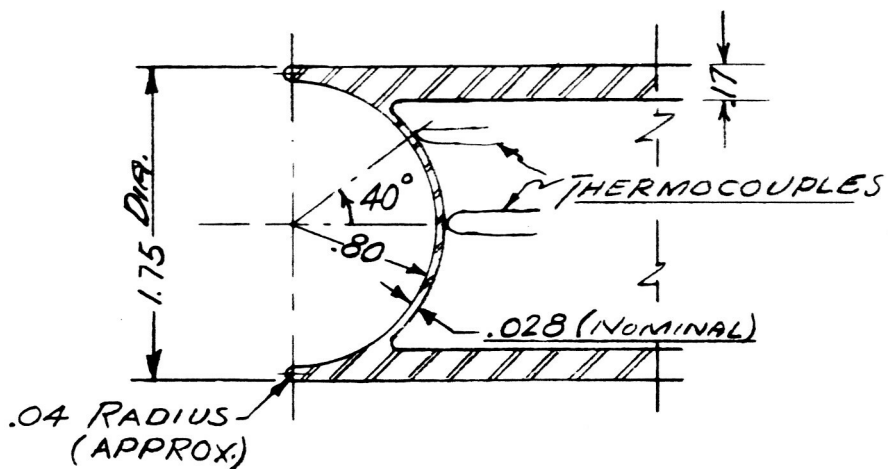
REFERENCES

1. Hopko, Russell N., and Strass, H. Kurt: Some Experimental Heating Data on Convex and Concave Hemispherical Nose Shapes and Hemispherical Depressions on a 30° Blunted Nose Cone. NACA RM L58A17a, 1958.
2. Markley, J. Thomas: Heat Transfer and Pressure Measurement on a 5-Inch Concave Nose at a Mach Number of 2.0. NACA RM L58C14a, 1958.
3. Maslen, Stephen H., and Moeckel, W. E.: Inviscid Hypersonic Flow Past Blunt Bodies. Preprint No. 665, S.M.F. Fund Preprint, Inst. Aero. Sci., Jan. 1957.
4. Boison, J. C., and Curtiss, H. A.: Preliminary Results of Spherical-Segment Blunt Body Pressure Surveys in the 20 Inch Supersonic Wind Tunnel at JPL. AVCO RAD Tech. Memo. 2-TM-57-77. (Aerod. Sec. Memo. No. 152), AVCO Res. and Advanced Dev. Div., Oct. 9, 1957.
5. Carslaw, H. S., and Jaeger, J. C.: Conduction of Heat in Solids. The Clarendon Press (Oxford), 1947.
6. Reshotko, Eli, and Cohen, Clarence B.: Heat Transfer at the Forward Stagnation Point of Blunt Bodies. NACA TN 3513, 1955.



(a) Photograph of model.

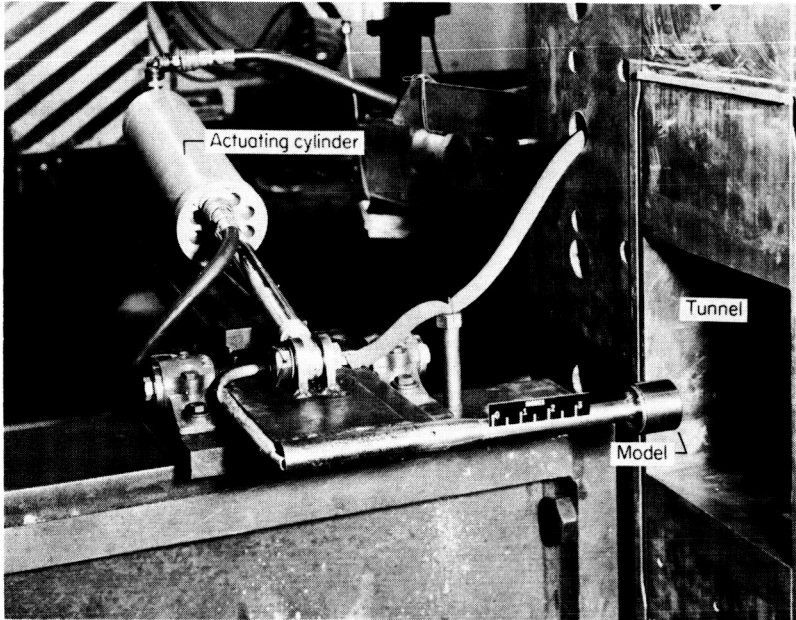
L-58-1627



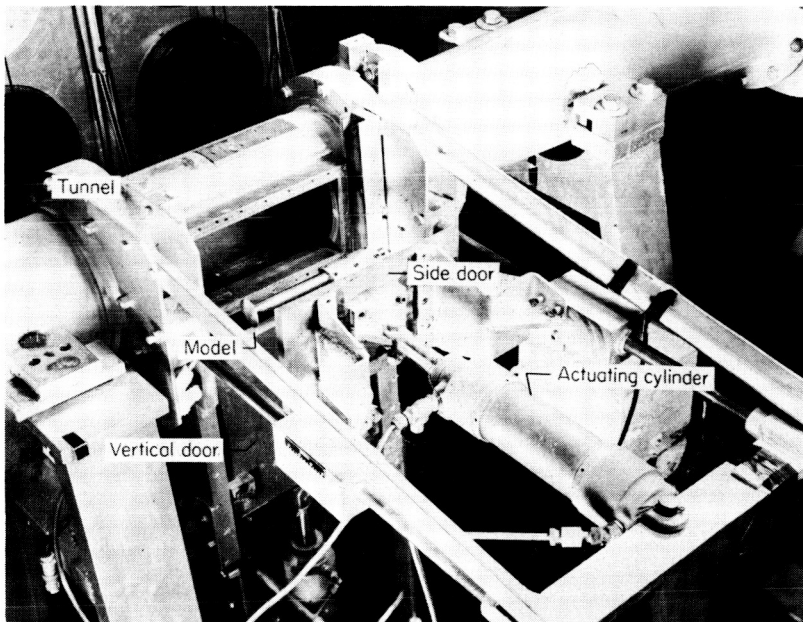
(b) Cross-section view of model. All dimensions in inches.

Figure 1.- Concave nose shape.





(a) $M = 1.98$.

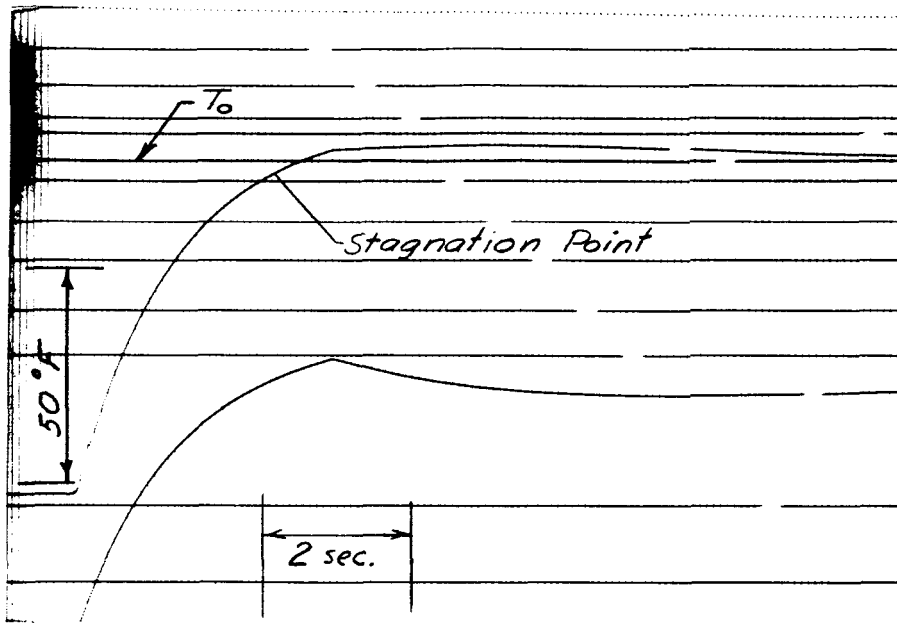


(b) $M = 4.95$.

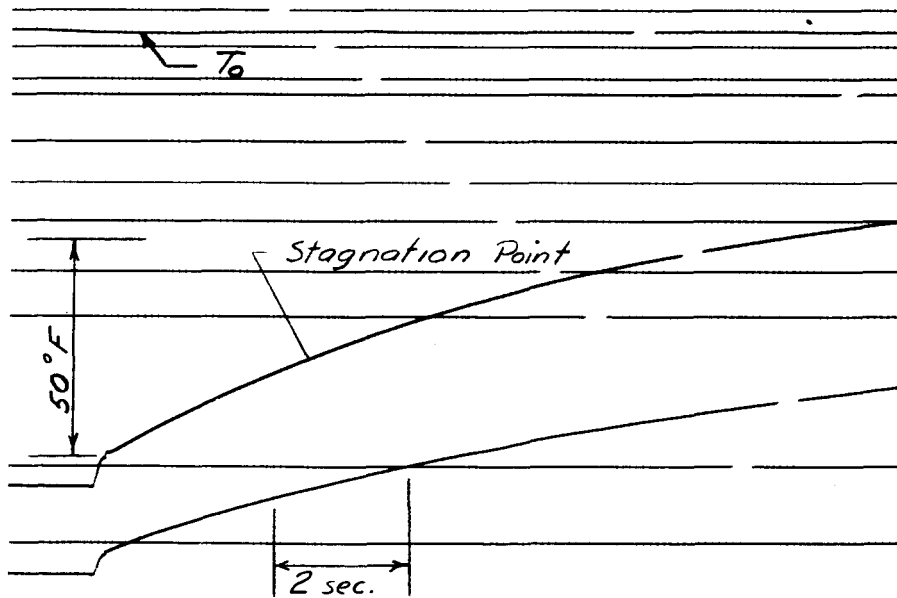
L-58-1628

Figure 2.- Photographs of installations.



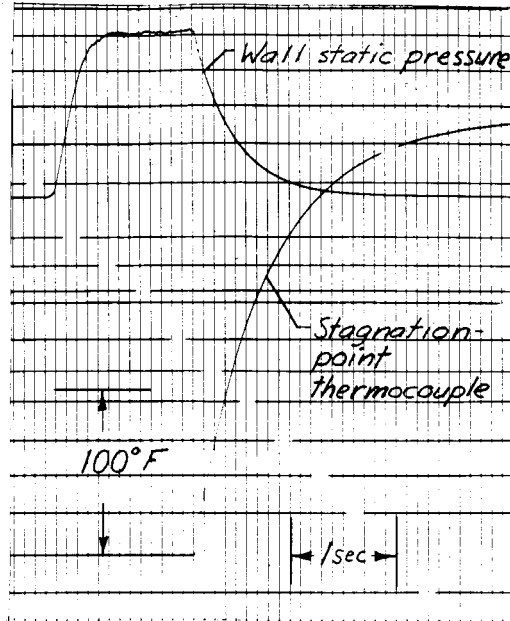


(a) High heat-transfer rate; $p_0 = 93$ lb/sq in. abs; $T_0 = 146^\circ$ F.

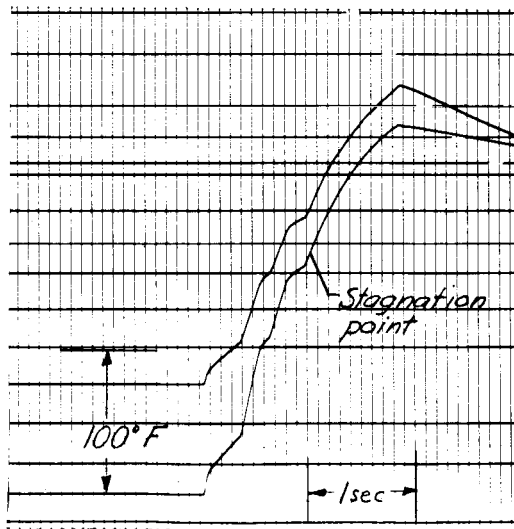


(b) Low heat-transfer rate; $p_0 = 92$ lb/sq in. abs; $T_0 = 154^\circ$ F.

Figure 3.- Typical thermocouple records showing high and low heat-transfer rates at $M = 1.98$, $\alpha \approx 0^\circ$, and $R_d \approx 3 \times 10^6$.

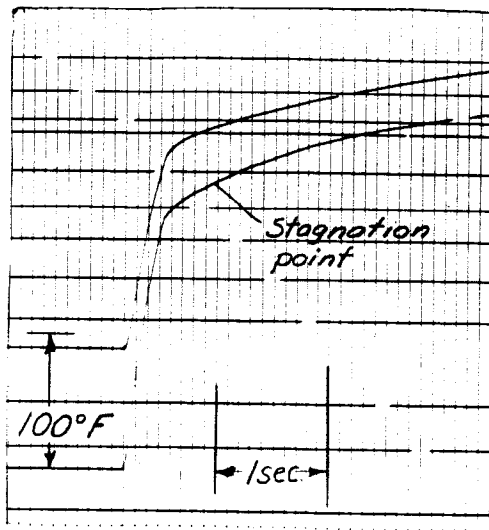


(a) High heat-transfer rate; $p_o = 1,025$ lb/sq in. abs; $T_o = 405^\circ$ F;
 $R_d = 4.4 \times 10^6$.

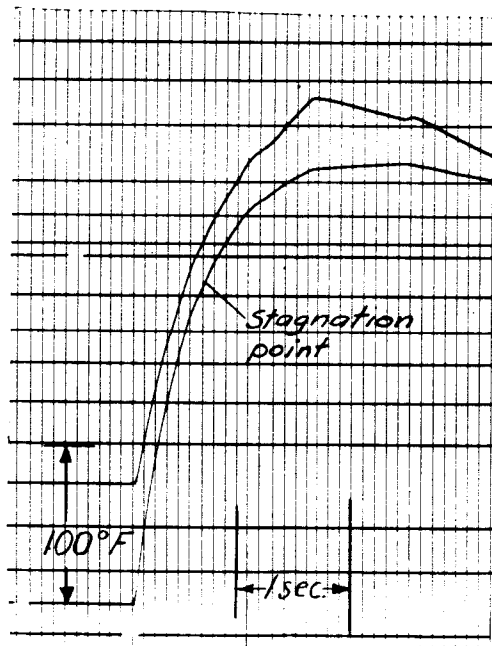


(b) Oscillating heat-transfer rate; $p_o = 1,020$ lb/sq in. abs;
 $T_o = 403^\circ$ F; $R_d = 4.4 \times 10^6$.

Figure 4.- Typical records showing the high, low, and oscillating heat rates at $M = 4.95$ and $\alpha \approx 0^\circ$.

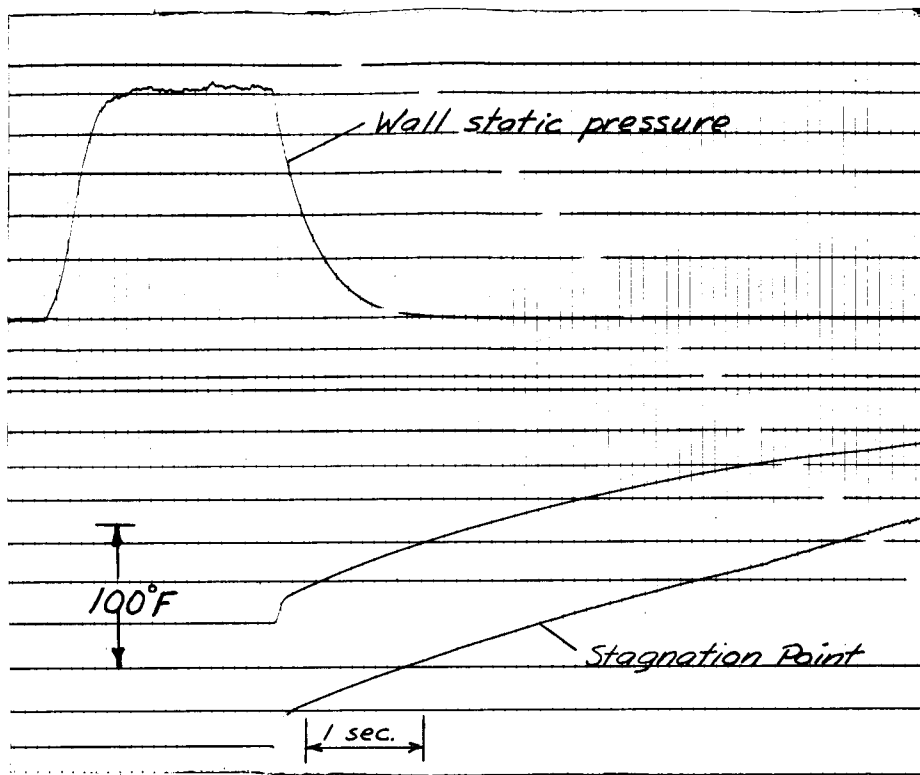


(c) High heat-transfer rate changing to low rate;
 $P_o = 2,535 \text{ lb/sq in. abs}$; $T_o = 402^\circ \text{ F}$; $R_d = 11 \times 10^6$.

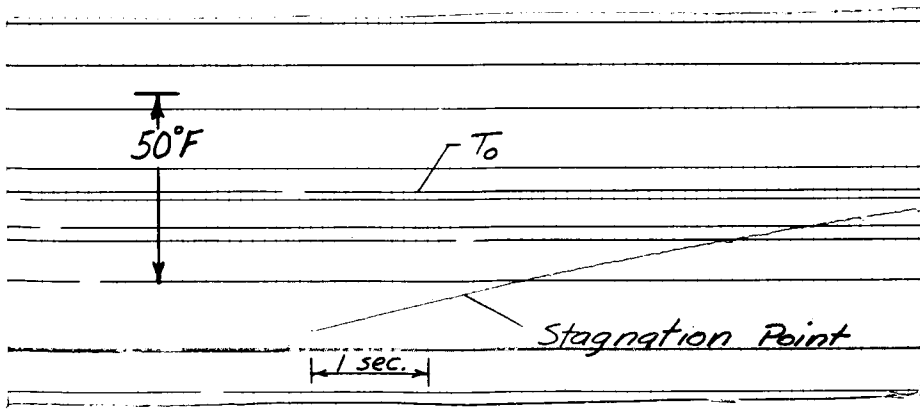


(d) High heat-transfer rate; $p_o = 1,515 \text{ lb/sq in. abs}$; $T_o = 398^\circ \text{ F}$;
 $R_d = 6.6 \times 10^6$.

Figure 4.- Concluded.



(a) $M = 4.95$; $\alpha = 10^{\circ}$; $p_o = 515 \text{ lb/sq in. abs}$; $T_o = 406^{\circ} \text{ F}$;
 $R_d = 2.2 \times 10^6$.



(b) $M = 1.98$; $\alpha \approx 2^{\circ}$; $p_o = 92 \text{ lb/sq in. abs}$; $T_o = 154^{\circ} \text{ F}$;
 $R_d = 3.1 \times 10^6$.

Figure 5.- Thermocouple records showing low heat-transfer rates at angle of attack.

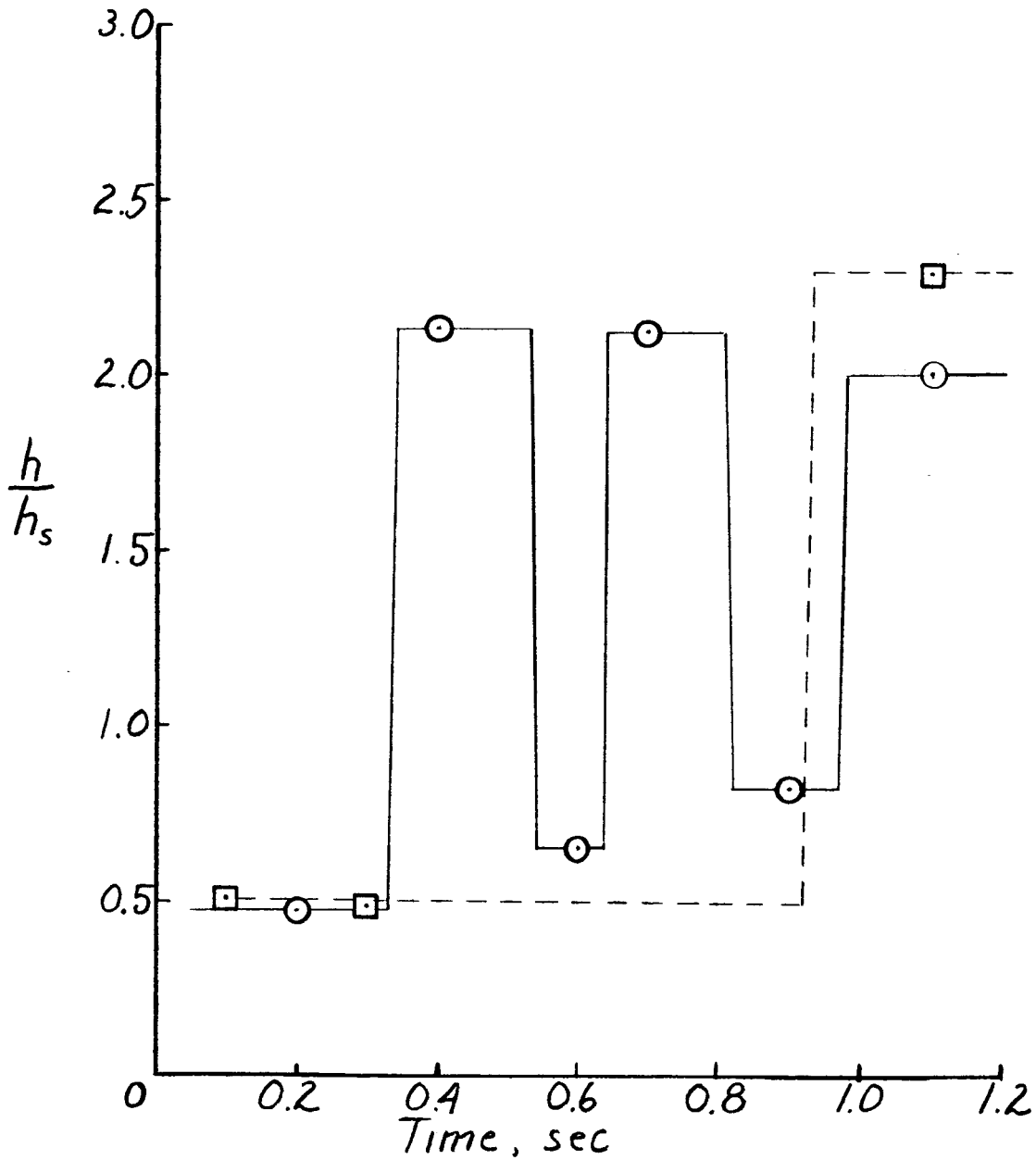
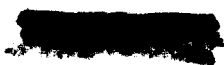


Figure 6.- Heat-transfer coefficient as function of time for oscillating flow. $M = 4.95$; $T_o \approx 400^\circ \text{ F}$; $R_d \approx 4.4 \times 10^6$. (Two runs shown.)



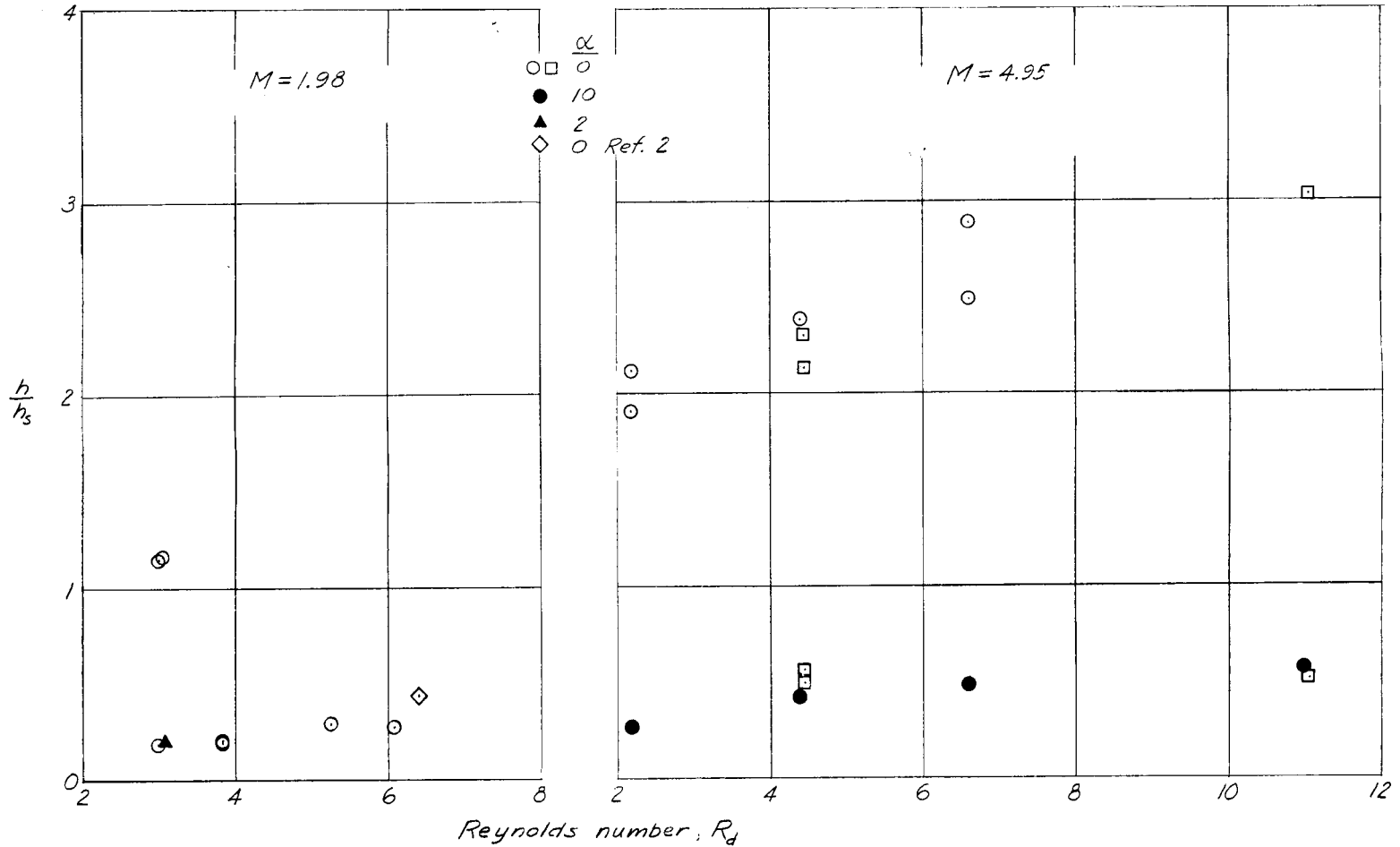
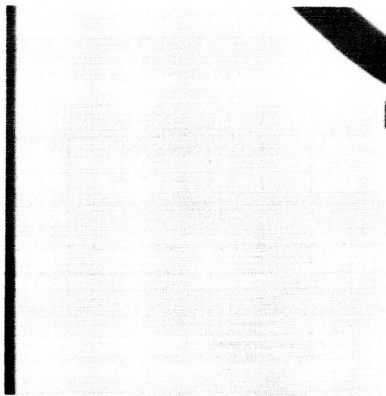
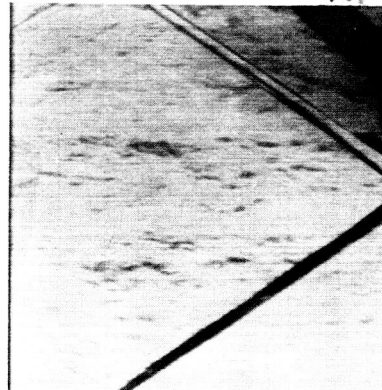


Figure 7.- Summary of heat-transfer-coefficient data. Square symbols indicate oscillating flow occurred during tests.



(a) No flow.



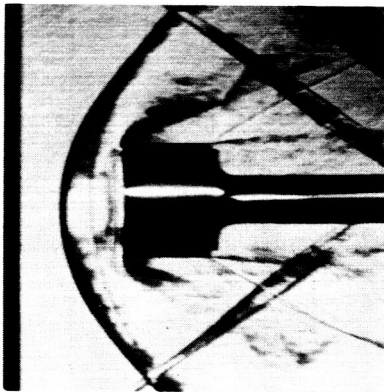
(b) Flow.



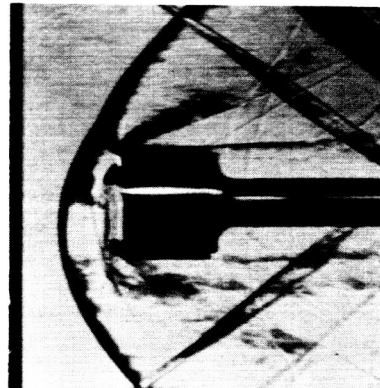
(c) Steady flow; $\alpha \approx 0^\circ$.



(d) Steady flow; $\alpha \approx 2^\circ$.



(e) Unsteady flow; $\alpha \approx 0^\circ$.



(f) Unsteady flow; $\alpha \approx 0^\circ$.

Figure 8.- Schlieren photographs illustrating the flow configurations. L-58-1629

$M = 1.98, R_d \approx 3 \times 10^6$.



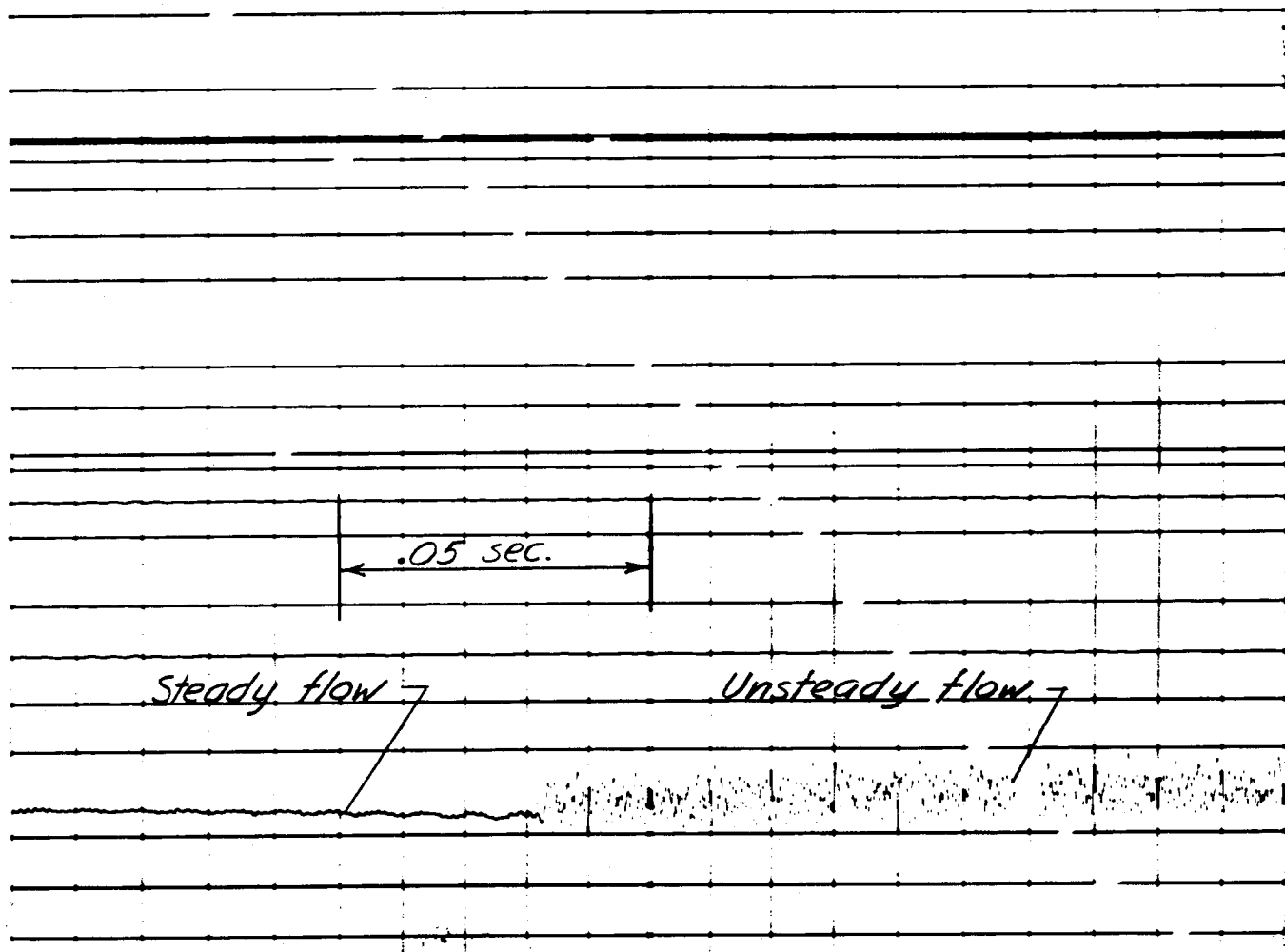


Figure 9.- Pressure fluctuations at stagnation point. $p_0 = 1,025$ lb/sq in. abs; $T_0 = 418^\circ$ F;
 $\alpha = 0^\circ$; $M = 4.95$.

CONFIDENTIAL

CONFIDENTIAL